

Low-temperature specific heat of an Fe₁₂ molecular cluster

M. Affronte,¹ J. C. Lasjaunias,² and G. L. Abbatì³

¹*I.N.F.M. - S³ National Research Center on nanoStructures and bioSystems at Surfaces and Dipartimento di Fisica, Università di Modena e Reggio Emilia, via G. Campi 213/A, I-41100 Modena, Italy*

²*Centre de Recherche sur les Très Basses Températures, C.N.R.S., BP166, F-38042 Grenoble Cédex 9, France*

³*I.N.S.T.M. and Dipartimento di Chimica, Università di Modena e Reggio Emilia, via G. Campi 183, I-41100 Modena, Italy*

(Received 22 August 2002; published 27 November 2002)

The pattern of the lowest-lying energy levels of Fe₁₂, a ferric wheel comprising $N=12$ antiferromagnetically coupled spins $s=5/2$, has been determined by specific-heat measurements between 0.5 and 10 K and in magnetic fields up to 7 T. Within the framework of a semiclassical model, we evaluated the parameters of the spin Hamiltonian: the exchange $J/k_B=37.60\pm 0.34$ K and the effective on-site anisotropy constant $k_z=0.46\pm 0.09$ K. The high value of the classical tunnel action $S_0/\hbar=Ns\sqrt{2k_z/J}=4.67$ estimated for Fe₁₂ suggests that favorable conditions for quantum tunneling of the Néel vector can be searched in large ferric wheels.

DOI: 10.1103/PhysRevB.66.180405

PACS number(s): 75.50.Xx, 75.40.Cx

Critical and quantum phenomena have been observed on a macroscopic scale¹ in molecular clusters, solid-state collections of identical, nanometer-sized magnets embedded in crystalline organic structures. Ring-shaped clusters¹ comprising antiferromagnetically coupled spins are a subgroup of this family of compounds and they can be considered as a prototype of single-molecule antiferromagnets in which quantum coherence² or level repulsion³ can be directly observed. Fe₆ (Ref. 4) and Fe₁₀ (Ref. 5) were the first ferric wheels to be synthesized and studied by different techniques such as NMR,⁶ torque magnetometry,⁷ and specific heat.⁸ Recently the larger molecular rings Fe₁₂ (Ref. 9) and Fe₁₈ (Ref. 10) have been synthesized. These successes in supramolecular engineering allow one to study the evolution from small rings to extended one-dimensional spin systems. The primary issue from both experimental and theoretical points of view is certainly the determination of the pattern of the energy levels. Since the intercluster interactions are in general very weak, the basic Hamiltonian for one ring is

$$H = \sum_{i=1}^N J_i \mathbf{s}_i \cdot \mathbf{s}_{i+1} + \sum_{i=1}^N U_i(\mathbf{s}_i) + \hbar \mathbf{h} \cdot \sum_{i=1}^N \mathbf{s}_i, \quad (1)$$

where N is the number of spins in the ring, $\mathbf{s}_1 = \mathbf{s}_{N+1}$, the J_i 's are antiferromagnetic Heisenberg interactions, and the final term is the Zeeman coupling with $\mathbf{h} = g\mu_B \mathbf{B}/\hbar$, where \mathbf{B} is an external magnetic field. The $U_i(\mathbf{s}_i)$ may contain all the intraring interactions (next-nearest neighbor, dipolar) and the single-ion anisotropy terms. For small and even N and in the limit of a strong exchange interaction, exact diagonalization of Eq. (1) shows that the singlet ground state, with total spin $S=0$ of the ring, is separated from the excited states $S=1, 2, 3$, etc. by energy gaps E_S that approximately follow the Landé interval rule $E_S \sim S(S+1)$.⁴ However, exact diagonalization of Eq. (1) for a system with just $N=12$ spins $s=5/2$ is beyond the possibilities of modern computation facilities. Schnack and Luban¹² have recently extended the validity of the Landé rule to cyclic systems with an odd number of sites as well as to all of the polytope configurations, and they refer to the excitations of a ring as a rotational band to stress the similarity with the energy spectrum of a rigid rotor.

Loss and co-workers considered the simplest case of constant J and a dominant uniaxial anisotropy so that contributions to the U term may be combined as a single anisotropy term $-k_z \sum_{i=1}^N s_{i,z}^2$ and the Hamiltonian (1) can be mapped to a form of the nonlinear σ model (NL σ M) for the staggered magnetization \mathbf{n} (Refs. 2 and 11) (the case a with more general form of magnetic anisotropy has been recently considered by Lü *et al.*¹³ and that with variable J by Meier and Loss¹⁴). Although the description of small clusters of $s=5/2$ spins in terms of NL σ M may be questionable (its limits are discussed in Ref. 14), this semiclassical approach has already been tested on the magnetization and torque results of Fe₆ and Fe₁₀ rings and it actually provides a good description of cyclic systems with generic N in terms of two parameters J and k_z of the spin Hamiltonian (1). Furthermore, Normand *et al.* provided a simple expression of the lowest-lying energy levels, and their zero-field splitting and magnetic-field dependence [see Eq. (5) of Ref. 11] are shown in Fig. 1. Most importantly, Loss and co-workers pointed out that fa-

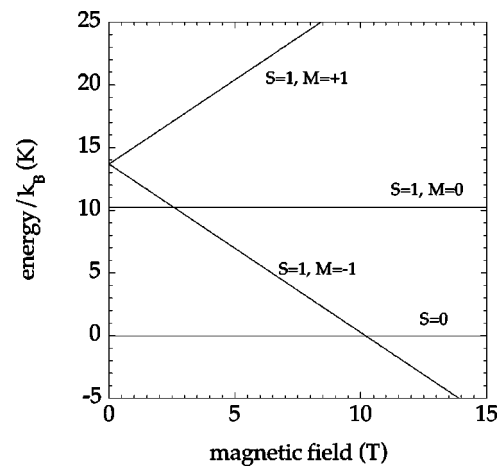


FIG. 1. Energy levels of Fe₁₂ estimated within the framework of the semiclassical approach [from Eq. (5) of Ref. 11]. Although the pattern of the lowest-lying levels is common for all the antiferromagnetically coupled ferric wheels, the J and k_z parameters used are those obtained in the present work.

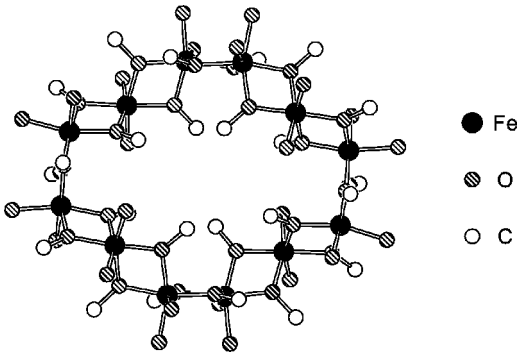
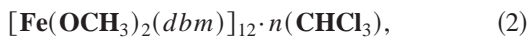


FIG. 2. Structure of the Fe_{12} core. Carbon-bonded oxygen atoms belong to methoxide groups, the free ones to *dbm* units.

favorable conditions for the coherent tunneling of the Néel vector \mathbf{n} between two degenerate states separated by an energy barrier² can occur in ferric wheels, so that a search for new candidates or strategies is highly desirable in this field. In this work we have used specific-heat measurements between 0.5 and 10 K and in magnetic fields up to 7 T to determine the J and k_z parameters of the spin Hamiltonian of Fe_{12} , among the largest ferric wheels reported so far.

Low-temperature heat-capacity measurements were performed by using a commercial Quantum Design PPMS with a ^3He cryogenic insert and a 7-T superconducting coil. This system automatically performs heat-capacity measurements by using the relaxation method and, below 2 K, a *two-tau* fitting method was used to extract heat-capacity values. Further measurements in zero field were also made by using the adiabatic method in a homemade cryostat. The background heat capacity of the microcalorimeter with 0.2 mg of Apiezon *N* grease used to glue the sample was measured in different magnetic fields and subtracted from the raw data.

The Fe_{12} compound was prepared as described in Ref. 9 and it has the chemical formula



where *dbm* is for the anion of dibenzoylmethane ($\text{Hdbm} = \text{C}_{15}\text{H}_{12}\text{O}_2$). Fe_{12} crystallizes in monoclinic space group $P2_1/c$ with unit-cell parameters $a = 30.530(5) \text{ \AA}$, $b = 22.780(5) \text{ \AA}$, $c = 32.050(5) \text{ \AA}$, $\beta = 93.400(5)^\circ$, and $V = 22251(7) \text{ \AA}^3$. The unit cell contains four Fe_{12} molecules related by an inversion center and a 2_1 screw axis, so that the iron clusters are not isooriented even in a single crystal. The molecular core structure (Fig. 2) comprises twelve iron (III) ions arranged to form a nonplanar ring (maximum departure from the mean plane $\pm 1.84 \text{ \AA}$) with a crystallographic C_1 point-group symmetry, but an idealized D_2 symmetry.⁹ One can define a z axis perpendicular to the mean plane of the iron ring but, since the crystal symmetry does not dictate dominant uniaxial anisotropy, hereafter k_z will be considered simply as an effective on-site parameter. The Fe_{12} crystal lattice also contains n disordered chloroform molecules which can be partially removed by vacuum treatment. Chemical analysis on pumped samples (approximately 0.1 torr for one hour) points to a residual chloroform content of

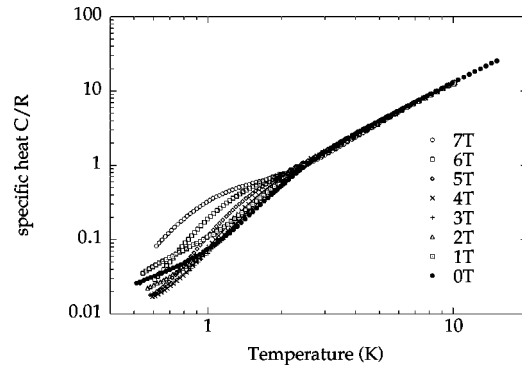


FIG. 3. The specific heat, normalized to the gas constant R , of an Fe_{12} molecular cluster in magnetic fields of 0–7 T.

$n = 2/3$ per Fe_{12} molecule. The molar weight is 4173.58 g/mol. Thin pellets of a few milligrams were prepared by pressing dried microcrystals.

We measured the heat capacity of five different samples and the results agree with each other both in amplitude (within 5%) and in shape. However, it is worth mentioning that the heat capacity of one sample was found to be much larger (about twice) than that for the others and we ascribe this to the fact that the drying procedure was not completed for this sample and it probably contained a large amount of solvent. In the following we concentrate on the set of data obtained on a thin pellet of 3.3 mg.

The temperature dependence of the specific heat, $C(T)$, normalized to the gas constant $R = 8.314 \text{ J/mol K}$, is plotted in Fig. 3 for different magnetic fields between 0 and 7 T. Data above $\sim 4 \text{ K}$ overlap while data obtained in different magnetic fields differ at low temperature, as a consequence of the shift of the main magnetic contribution towards lower temperature as the magnetic field increases. One further feature is worth noting: the $C(T)$ curves obtained at low fields, $B = 0, 1, \text{ and } 2 \text{ T}$, show a further increase below $\sim 1 \text{ K}$. This suggests the presence of a low-temperature anomaly that should be taken into account in the data analysis. Bearing these features in mind, we consider three contributions to the specific heat of Fe_{12} : the lattice contribution C_{latt} , the magnetic contribution C_m due to the energy gap between the ground and the excited states of the Fe_{12} molecule, and finally a two-level Schottky contribution C_{Sch} that accounts for the low-temperature anomaly, i.e., $C = C_{latt} + C_m + C_{Sch}$. We already observed in a previous work¹⁵ that the Debye temperature Θ_D is, in general, very low for molecular crystals, and correction terms to the $\sim T^3$ Debye law are necessary even at low temperatures. Therefore, we consider the following expression:¹⁵

$$C_{latt}/R = \frac{234rT^3}{(\Theta_D + \delta T^2)^3},$$

where r is the number of atoms per molecule (471 in our case). Values of Θ_D and δ are first determined by fitting the $C(T)$ data above $\sim 4 \text{ K}$ and then refined by the overall best

least-squares fitting procedure. The magnetic term $C_m/R\beta^2$ of a system having a set of energy levels ϵ_i can be expressed as

$$\frac{\sum_i \epsilon_i^2 \exp(-\beta \epsilon_i) \sum_i \exp(-\beta \epsilon_i) - [\sum_i \epsilon_i \exp(-\beta \epsilon_i)]^2}{[\sum_i \exp(-\beta \epsilon_i)]^2},$$

which is essentially the Schottky law extended to a multi-level system, with $\beta = (k_B T)^{-1}$. We consider the energy levels $E_{1,0}$ and $E_{1,\pm 1}$ of the triplet state described in the framework of the semiclassical model [see Eq. (5) of Ref. 11] as compared to the ground state $E_{0,0}$ while higher levels are neglected since their effects are masked by the lattice contribution at high temperatures. Since we deal with randomly oriented rings, we can average the dependence on the angle ψ between the z axis and the magnetic-field direction between 0 and π , so that

$$\epsilon_0 = E_{1,0} - E_{0,0} = 4J/N - \frac{1}{15} N k_z s^2, \quad (3)$$

$$\epsilon_{\pm 1} = E_{1,\pm 1} - E_{0,0} = 4J/N + \frac{1}{30} N k_z s^2 \pm \mu_B g B \quad (4)$$

with $g = 2$. In such a way, the pattern of the low-lying energy levels is determined by two parameters J and k_z that are evaluated by the simultaneous best fit of different $C(T)$ curves with different B values. In practice, J and k_z are first determined by fitting the $C(T)$ data obtained in zero field and $B = 7$ T and further refined fitting the $C(T)$ data obtained at intermediate-field values. In this way the fitting procedure rapidly converges.

The origin of the low-temperature anomaly is probably related to the presence of magnetic impurities or defective rings since spurious paramagnetic contributions have been also detected by the low-temperature susceptibility.⁹ We consider a simple two-level Schottky law:

$$C_{Sch}/R = \frac{g_0}{g_1} \left(\frac{T_0}{T} \right)^2 \frac{\exp(T_0/T)}{[(g_0/g_1) \exp(T_0/T) + 1]^2}$$

and we allow the parameter T_0 to change as the magnetic field increases while the (g_0/g_1) ratio is determined by the best fit of low-temperature data at $B = 0 - 2$ T: we found $(g_0/g_1) = 11.7 \pm 1$. Such a high value of (g_0/g_1) is required to account for the small amplitude of the anomaly and it could be related to high degeneracy or, more likely, it simply indicates that only a small fraction ($< 10\%$) of the sample is involved. The nonlinear field dependence of T_0 (see Table I) points to a nontrivial level splitting reminding the behavior of anisotropic paramagnetic defects in a field perpendicular to the principal molecular magnetic axis.

The overall best least-squares fit gives $\Theta_D = 150.1$ K, $\delta = 0.595$ K⁻¹, $J/k_B = 37.60 \pm 0.34$ K, and $k_z = 0.46 \pm 0.09$ K. Detailed results are also reported in Table I. It is worth noting that since both the experimental data and theoretical curves are referred to one mole, the comparison is direct with no adjustable factors. In Figs. 4(a) and 4(b) we show the $C(T)$ experimental data compared with the fitting

TABLE I. Results of best-least squares fit of the $C(T)$ curves obtained in different magnetic fields. For all the curves $\Theta_D = 150.1$ K, $\delta = 0.595$ K⁻¹, $(g_0/g_1) = 12$ while χ^2 shows the fit quality.

T	J/k_B (K)	k_z (K)	T_0 (K)	χ^2
0	37.88	0.550	2.584	0.828
1	37.35	0.471	2.550	1.699
2	37.37	0.584	3.132	1.603
3	38.13	0.491	3.545	1.555
4	37.72	0.469	5.811	1.429
5	37.95	0.295	6.161	1.658
6	37.14	0.310	7.811	1.174
7	37.28	0.480	12.05	1.616

results for $B = 0$ T and 7 T respectively. The individual component contributions are also plotted in these figures. We note that for $B = 0$ T, C_m is comparable to C_{latt} at ~ 3 K but the latter dominates for $T \geq 4$ as expected. The hump in $C_m(B = 0$ T) at $T \sim 3.5$ K $\ll J/k_B$ is a characteristic of finite systems, not found in the case of the infinite Heisenberg $s = 5/2$ chain¹⁷ and this is due to the opening of a gap in the energy spectrum. For $B = 7$ T, this hump is shifted towards lower temperatures and C_m is larger than C_{latt} below ~ 3 K. $C_{Sch}(B = 0$ T) has its maximum at ~ 1 K and it contributes significantly at low T and low B , but T_0 is shifted towards high temperatures as the field increases so that $C_{Sch}(B = 7$ T) contributes very little to the total specific heat. The pattern of the lowest-lying energy levels thus determined for Fe₁₂ is plotted in Fig. 1.

In a previous work⁹ a study of the temperature dependence of the magnetic susceptibility between 2.3 and 254 K led to the evaluation of an exchange constant $J/k_B = 31.9$ K ($J = 22.2$ cm⁻¹) assuming a Heisenberg $s = 5/2$ quantum chain model for Fe₁₂. This can be compared with the results

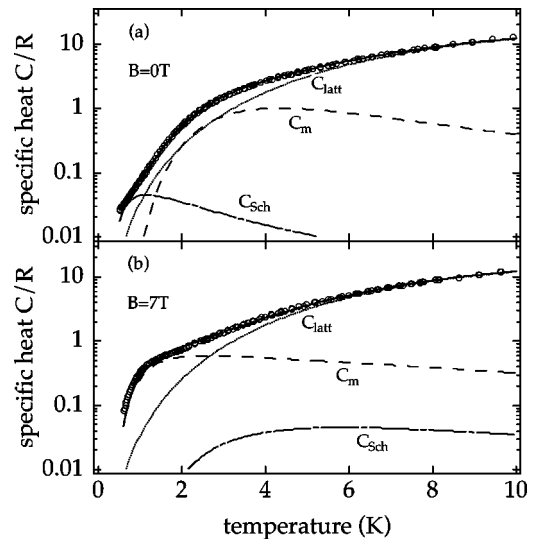


FIG. 4. The specific heat of Fe₁₂ measured at zero field (a) and at 7 T (b). Data fitting and individual component contributions are also plotted.

reported here, taking into account that the evaluation of J was obtained at high temperature and it did not account for finite-size effects and anisotropy. Although we did not reach the crossing field, we may evaluate B_{c1} by imposing $E_{1,-1} = E_{0,0}$, i.e., from Eq. (6) of Ref. 11:

$$B_{c1} = \frac{4J}{g\mu_B N} \left[1 + \frac{k_z N^2 s^2}{30J} \frac{1}{4} \right] = 10.17 \text{ T}. \quad (5)$$

This value is in excellent agreement with preliminary measurements of the magnetization up to 50 T performed at 1.3 K on an Fe₁₂ polycrystalline sample that directly measured a critical field $B_{c1} = 10.0 \pm 0.5$ T.¹⁶ It is worth noting that specific-heat measurements in zero field are unable on their own to distinguish between positive or negative k_z values since the pattern of the energy levels is equivalent in these two cases. Fortunately, this is no longer true once the magnetic field is applied (see Fig. 1) so that the sign of k_z is determined by the magnetic-field dependence of C_m , in spite of the fact that polycrystalline samples were used. Since C_m is masked to a large extent by C_{latt} , we believe that a model with more parameters (considering, for instance, different

anisotropy configurations) would provide ambiguous fitting parameters. In this respect, we may conclude that the approximations used in the semiclassical approach are suitable to describe the thermodynamic properties of the ferric wheels well. Finally, it is interesting to evaluate the classical tunnel action $S_0/\hbar = N_S \sqrt{2k_z/J}$ for Fe₁₂ since this must be sufficiently large ($S_0/\hbar \gg 2$) in order to have a well-localized Néel vector along the z -direction.¹⁴ For Fe₁₂ we find $S_0/\hbar = 4.67$ which is the highest value among the ferric wheels studied so far ($S_0/\hbar = 2.47$ and 3.32 for Fe₆ and Fe₁₀ respectively, see Table I in Ref. 14). Although high quality Fe₁₂ crystals with a good alignment of rings and small decoherence factors are unavailable at the moment, we may conclude that the high S_0/\hbar estimated for Fe₁₂ suggests that large ferric wheels may be good candidates for the tunnel scenario proposed by Loss and co-workers.

We thank A. Cornia (Modena), A. Caneschi, and D. Gatteschi (Florence) for encouraging work on large ferric wheels and sharing results with us. Special thanks also to A. Bilusic (Zagreb) for his contribution to the specific-heat measurements.

-
- ¹See, e.g., A. Caneschi, D. Gatteschi, C. Sangregorio, R. Sessoli, L. Sorace, A. Cornia, M.A. Novak, C. Paulsen, and W. Wernsdorfer, *J. Magn. Magn. Mater.* **200**, 182 (1999), and references therein.
- ²A. Chiolero and D. Loss, *Phys. Rev. Lett.* **80**, 169 (1998); F. Meier and D. Loss, *ibid.* **86**, 5373 (2001).
- ³M. Affronte, A. Cornia, A. Lascialfari, B. Borsa, D. Gatteschi, J. Hinderer, M. Horvatić, A.G.M. Jansen, and M.H. Juliet, *Phys. Rev. Lett.* **88**, 167201 (2002).
- ⁴A. Caneschi, A. Cornia, A.C. Fabretti, S. Foner, D. Gatteschi, R. Grandi, and L. Schenetti, *Chem.-Eur. J.* **2**, 1379 (1996); G.L. Abbati, A. Caneschi, A. Cornia, A.C. Fabretti, D. Gatteschi, W. Malavasi, and L. Schenetti, *Inorg. Chem.* **36**, 6443 (1997).
- ⁵K.L. Taft, C.D. Delfs, G.C. Papefthymiou, S. Foner, D. Gatteschi, and S.J. Lippard, *J. Am. Chem. Soc.* **116**, 823 (1994).
- ⁶M.-H. Julien, Z.H. Jang, A. Lascialfari, F. Borsa, M. Horvatić, A. Caneschi, and D. Gatteschi, *Phys. Rev. Lett.* **83**, 227 (1999).
- ⁷A. Cornia, A.G.M. Jansen, and M. Affronte, *Phys. Rev. B* **60**, 12 177 (1999); A. Cornia, A.G.M. Jansen, M. Affronte, G.L. Abbati, and D. Gatteschi, *Angew. Chem. Int. Ed. Engl.* **38**, 2264 (1999).
- ⁸M. Affronte, J.C. Lasjaunias, A. Cornia, and A. Caneschi, *Phys. Rev. B* **60**, 1161 (1999).
- ⁹A. Caneschi, A. Cornia, A.C. Fabretti, and D. Gatteschi, *Angew. Chem. Int. Ed. Engl.* **39**, 1295 (1999); G.L. Abbati, A. Caneschi, A. Cornia, A.C. Fabretti, and D. Gatteschi, *Inorg. Chim. Acta* **297**, 291 (2000).
- ¹⁰S.P. Watton, P. Fuhrmann, L.E. Pence, A. Caneschi, A. Cornia, G.L. Abbati, and S.J. Lippard, *Angew. Chem. Int. Ed. Engl.* **36**, 2774 (1997).
- ¹¹B. Normand, X. Wang, X. Zotos, and D. Loss, *Phys. Rev. B* **63**, 184409 (2001).
- ¹²J. Schnack and M. Luban, *Phys. Rev. B* **63**, 014418 (2000).
- ¹³Rong Lü, Jia-Lin Zhu, Yi Zhou, and Bing-Lin Gu, *Phys. Rev. B* **64**, 064423 (2001).
- ¹⁴F. Meier and D. Loss, *Phys. Rev. B* **64**, 224411 (2001).
- ¹⁵M. Affronte, J.C. Lasjaunias, and A. Cornia, *Eur. Phys. J. B* **15**, 633 (2000).
- ¹⁶A. Cornia (private communication).
- ¹⁷W.J.M. deJonge, C.H.W. Swüste, K. Kopinga, and K. Takeda, *Phys. Rev. B* **12**, 5858 (1975).